Dicing Process for the Device Separation of a Slider with an Integrated Microactuator (SLIM)

S. Cvetkovic, H. Saalfeld, and H.H. Gatzen
Institute for Microtechnology
Center for Production Technology
Leibniz Universität Hannover
Garbsen, Lower Saxony, Germany

ABSTRACT
A Micro Electro-mechanical Systems (MEMS) type Slider with an Integrated Microactuator (SLIM) is capable of moving the read-write element both in vertical direction (adjusting the flying height) and in lateral direction (allowing second stage actuation). Developing this system not only poses substantial challenges in the area of wafer processes, but also in mechanical micromachining for separating the parts. The main challenge is to release a mounting block without breaking the delicate Si leaf springs it is suspended on. This paper describes the process development for separating Si stacks with parts suspended on delicate solid state joints, ultimately intended for being applied to machining the SLIM device. It presents the slicing and dicing experiments conducted and outlines the results.

INTRODUCTION
To increase the recording density of Hard Disc Drives (HDD), a second stage actuator may be integrated in the read/write head to accomplish more accurate and higher frequency track following than possible with existing actuators [1, 2]. One cost competitive approach to achieve this goal is implementing a Slider with an Integrated Microactuator (SLIM) as shown in Fig. 1 [3].

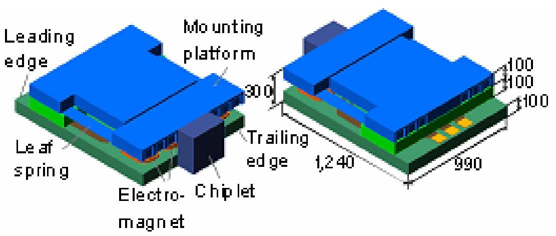

FIGURE 1. Slider with an Integrated Microactuator (SLIM)

An integrated microactuator activates a mounting block to which a chiplet containing the read-write element is attached. The actuator is capable of moving the read-write element on the chiplet both in vertical direction (adjusting the flying height) and in lateral direction (allowing second stage actuation). The mounting block is suspended by a pair of Si leaf springs.

The SLIM is fabricated on two separate wafers. The actuator micro magnetics are located in the bottom part of the device and consist of a pair of active parts. The actuator micro mechanics on top of the micro magnetics part include (1) a base, (2) an actuated mounting platform to which the read/write element (residing on a chiplet) will be mounted, and (3) a pair of Si leaf springs connecting both. A spacer joins the bottom and the top. Each of the three pieces (bottom, top, and spacer) is 100 µm thick; therefore, the whole slider body is a 300 µm thick, stacked structure.

As already mentioned, the SLIM micro magnetics and micro mechanics are fabricated in two separate wafer processes. After their completion, both types of wafers are separated into double row bars. A double row bar consists of two rows of ten slider each, with the sliders joined at their leading edge. The dimensions of either one are 11.89 mm x 2.6 mm x 0.1 mm. The row bars with the mechanics feature anchors for the mounting block at either end. This is necessary for immobilizing the leaf springs until a final slider separation takes place.

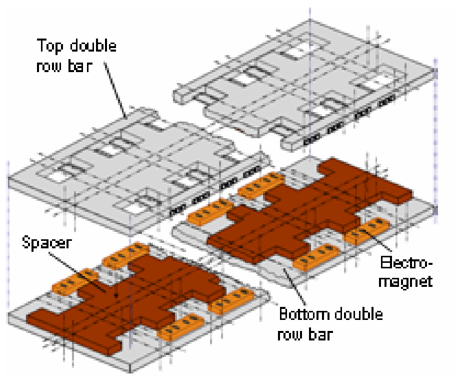

FIGURE 2. Double row bar level stacking (Step 1 and 2)

The fabrication process after dicing the two wafers is as follows. The micro magnetics and micro mechanics double row bars are joined by stacking them with a spacer sandwiched in between (Step 1). After the stacking, the chiplets are attached (Step 2) (Fig. 2). Next, the contact pads at the SLIM leading edges are released by slicing the top of the stacked double row bars (Step 3) (Fig. 3a). After this process step, the double row bar is debonded and remounted topside down. A slicing cut through the double row bar's bottom causes a separation into single row bars (Step 4) (Fig. 3b). However, no debonding occurs at this stage. For separating the sliders, the row bars are sliced (Step 5) (Fig. 3c). A further debonding process releases the single SLIM elements (Step 6). The final two steps are particularly sensitive, since they release the mounting block suspended by the delicate Si leaf springs.

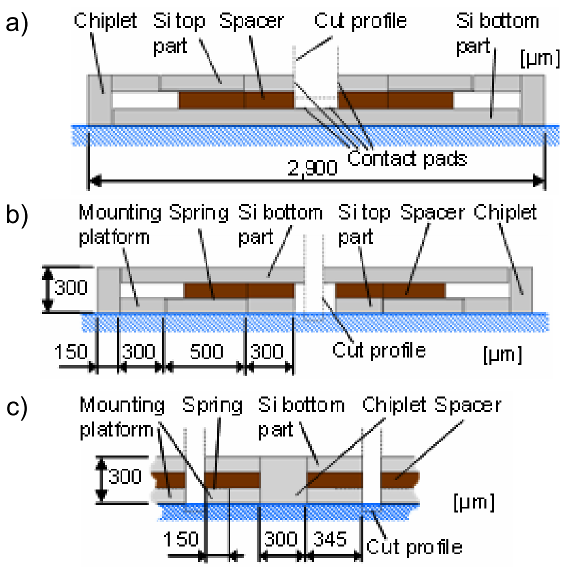

FIGURE 3. Double row bar machining. a) Cut for releasing the contact pads (Step 3); b) Cross cut for creating single row bars (Step 4); and c) dicing cut for slider release (Step 5)

This device poses some interesting machining challenges typical for stacked MEMS devices with cantilever suspended parts released by a dicing process. Besides machining stacked devices without excessive chipping, parts suspended on delicate cantilevers are released by the machining step. This requires a sufficient adhesion of the part during machining, as well as a gentle debonding process to avoid breakage of the delicate cantilevers while the parts are released. The purpose of this paper is to investigate these machining challenges.

EXPERIMENTAL

Starting point for the Si machining tests were studies performed previously [4, 5]. Si can be diced rather easily since it is subject to a metal transition under the pressure conditions occurring during the dicing [6].

Cutting Parameters

Table 1 presents the cutting parameters applied. For the dicing process, four types of dicing wheels were utilized: one with a Ni and the other three with bronze binders of three different hardnesses. The feed rate was varied, and the influence of the coolant supply on both the adhesion of the samples and the integrity on the cantilevers was observed. All parameter combinations were investigated; for each combination, three cuts were made.

TABLE 1. Dicing parameters

Feed rate [mm/min]	1	5	10	-
Binder type	Ni hard	Bronze hard	Bronze medium hard	Bronze soft
Wheel width [µm] (mounting block size)	15	45	100	-
Wheel width [µm] (row bar machining)	100			
Grit size [µm]	4-6			

Dicing was done using a DAC551 dicing machine with a positional accuracy of 0.2 µm and a spindle speed of 30,000 RPM, located in an air conditioned room.
Table 2 provides an overview over the bonding tapes used. Three bonding tapes, differing in the respective adhesive force, were evaluated: a standard "blue tape", a UV-release tape, and thermo-release tape.

TABLE 2. Dicing tape parameters

Dicing tape	Thickness [µm]	Adhesive strength [N/20 mm]	
		Nominal	Releasing
Nitto SWT 20+ (blue tape)	65	0.70	
Nitto UE-111 AJ (UV-tape)	110	8.33	0.20
REXPAN RP3 (thermo-release tape)	211	5.80	0

Mounting Block Size Investigations

Bond issues typically affect the MEMS design, therefore they have to be taken into account appropriately. In our case, the minimal required contact area of the mounting block had to be determined. For avoiding a parts tear-off, the following conditions have to be met: the forces the mounting block is subjected to during the machining process have to be smaller than the adhesive forces exerted by the bonding tape the slider is mounted on. The cutting force exerted is a function of the substrate thickness, the wheel width, and the general cutting parameters. These forces have to be counterbalanced by the tape adhesive force, which is dependent on the tape type and the contact area. Therefore, as a part of a MEMS design process, investigations regarding the contact area required for a save bond have to be conducted.

Double Row Bar Separation Investigations

For simulating MEMS stacks, stacked Si test structures were used (Fig. 4). Two types of Si stacks were applied. Type 1 was a double stack as found in double row bar slicing. Type 2 was a triple stack to simulate slider separation (Step 5).

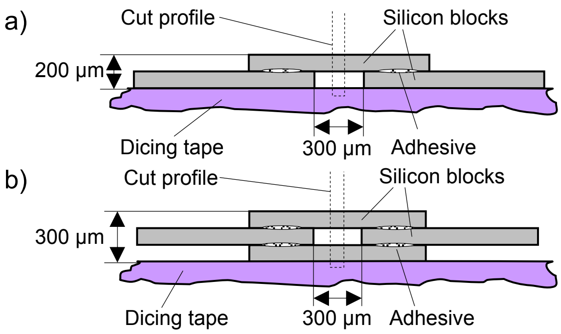

FIGURE 4. Si stacks used in the investigations. a) Si stack to simulate double row bar separation (Type 1); b) Si stack to simulate slider separation (Type 2)

RESULTS

Mounting Block Size Investigations

Table 3 presents the results for the adhesion tests. The test results are shown for two test block footprints: 300 µm x 300 µm and 100 µm x 100 µm. Tests were considered successful (A), if all blocks were still found on the tape after dicing. Tests were considered partly successful (B) if at least 50% of the blocks remained on the tape. Tests failed (C), if less then 50% of the blocks remained on the tape.

TABLE 3. Adhesion results for various blocks

Block footprint [µm]		300 x 300								
Block thickness [µm]		100			300			525		
Wheel width [µm]		15	45	100	15	45	100	15	45	100
Dicing tape	Blue	A	A	B	A	B	B	-	B	B
	UV	A	A	A	A	A	A	-	A	B
	Thermo	A	A	A	A	A	A	-	A	B
Block footprint [µm]		100 x 100								
Block thickness [µm]		100			300			525		
Wheel width [µm]		15	45	100	15	45	100	15	45	100
Dicing tape	Blue	A	B	C	B	B	C	-	B	C
	UV	A	A	B	A	A	B	-	A	B
	Thermo	A	A	B	A	A	B	-	A	B
A: successful; B: partly-successful; C: failed										

The effect of the coolant supply was investigated by covering the substrate with a blue tape. The number of retained parts could thus be enhanced by 10 to 20%.
After the completion of the test series, the actual desired shape of the mounting block was taken into consideration. The smallest block footprint that could be successfully diced was 500 µm x 100 µm (Fig. 5). The usage of UV or thermo-release tapes in combination with a wide wheel yielded the best results.

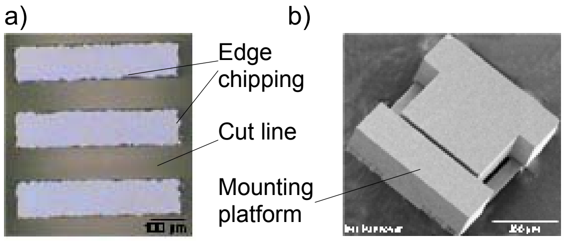

FIGURE 5. Mounting block size results. a) 500 µm x 100 µm blocks; b) 990 µm x 300 µm prototype of mounting platform

To assure that dicing and releasing the parts with free floating thin Si cantilever does not lead to the breakage (simulating Step 5); blocks featuring U-shaped cuts simulating delicate solid state joints were subjected to cutting tests. A thermo-release tape debonding at 140°C proved to be capable of releasing such delicate structures.

Double Row Bar Separation Investigations

Figure 6 depicts the results for the maximal edge chipping, while Fig. 7 shows the achieved cut width. A minimal edge chipping, but also the highest sensitivity to the feed rate was observed using a dicing wheel with a soft bronze binder. The optimal cut width was achieved using the hardest Ni bonded wheel.

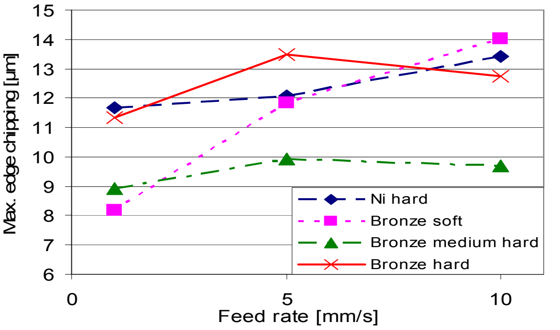

FIGURE 6. Dependence of feed rate and edge chipping for different dicing wheels

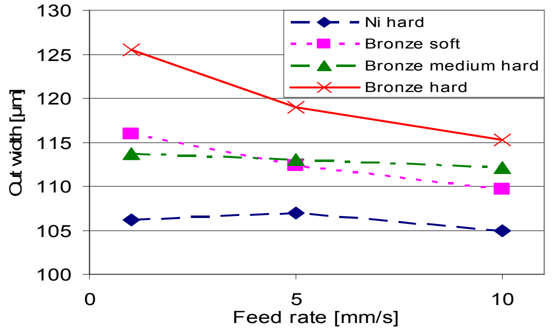

FIGURE 7. Dependence of feed rate and cut width for different dicing wheels

These results indicate that the lowest edge chipping can be achieved using wheels with a soft bond and a low feed rate. On the other hand, wheels with a hard bond are capable of achieving a minimal cut width and are less sensible in regard to the feed rate.

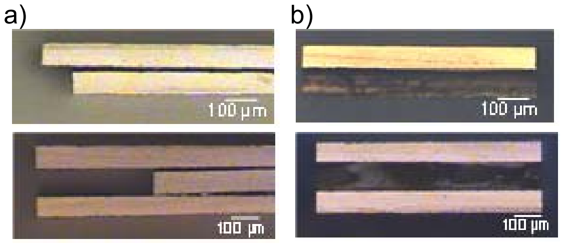

FIGURE 8. Diced and released stacked Si structures: a) side and b) front view

The next task was to find optimal parameters to dice and separate the parts simulating Steps 4 and 5. Using UV and thermo-release tapes, a coolant supply cover and a wheel with 45 µm width as well as a feed rate of 5 mm/s all of the stacked structures could be diced and released from the tape (Fig. 8). All chipping was below critical values, thus not jeopardizing the functionality of the parts (Fig 9).

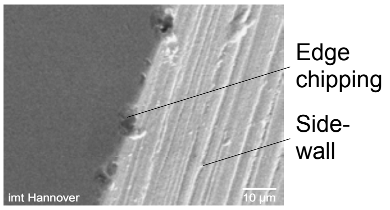

FIGURE 9. SEM-micrograph of edge chipping:

CONCLUSIONS AND OUTLOOK

One particular machining challenge is to separate MEMS stacks, especially if the separation cut includes releasing component parts suspended on delicate cantilevers. With optimal dicing parameters, Si stacks could be diced successfully. A non-destructive debonding of solid state joints could be achieved by using a thermo-release tape. Based on these investigations, a dicing process for stacked SLIM device will be developed and executed.

REFERENCES

[1] L.-S. Fan, et al. "Magnetic Recording Head Positioning at Very High Track Densities Using a Microactuator-Based, Two-stage Servo System", IEEE Trans. Industrial Electronics, 42(3), pp. 222-233, 1995

[2] Y. Lu, et al., „A Silicon Microactuator Using Integrated Microfabrication Technology", IEEE Trans. Mag., 39(5), pp. 2240-2242, 2003

[3] H.H. Gatzen, et al. A Slider with an Integrated Microactuator (SLIM) for Second Stage Actuation in Hard Disc Drives, Intermag, Madrid 2008, Accepted for IEEE Trans. on Magnetics

[4] M. Shikida, et al. Fabrication of Densely Arrayed Micro-Needles with Flow Channels by Mechanical Dicing and Anisotropic Wet Etching, J. Micromech. Microeng., Vol. 16, pp. 1740–1747, 2006

[5] H.H. Gatzen, S. Cvetkovic. Effect of Feed Rate and Grain Concentration on Ductile to Brittle Transition by Silicon Dicing, Proc. Euspen 7th Int. Conf. 2007, Bremen, Germany, Vol. 2, pp. 380-383, 2007

[6] J. Patten et al. Nanoindentation Tests on Diamond-machined Silicon Wafers, App. Phys. Lett. 86, pp. 181913-1-3, 2005